Simultaneous Multi-Region Detection of GABA+ and Glx using 3D Spatially Resolved SLOW-editing and EPSI-readout at 7T

Guodong Weng , Johannes Slotboom , Philippe Schucht , Ekin Ermiş , Roland Wiest , Stefan Klöppel , Jessica Peter , Irena Zubak , Piotr Radojewski

PII: S1053-8119(24)00006-5
DOI: https://doi.org/10.1016/j.neuroimage.2024.120511
Reference: YNIMG 120511

To appear in: *NeuroImage*

Received date: 29 September 2023
Revised date: 7 December 2023
Accepted date: 4 January 2024

Please cite this article as: Guodong Weng , Johannes Slotboom , Philippe Schucht , Ekin Ermiş , Roland Wiest , Stefan Klöppel , Jessica Peter , Irena Zubak , Piotr Radojewski , Simultaneous Multi-Region Detection of GABA+ and Glx using 3D Spatially Resolved SLOW-editing and EPSI-readout at 7T, *NeuroImage* (2024), doi: https://doi.org/10.1016/j.neuroimage.2024.120511

Highlights

- Novel SLOW-EPSI technique for accurate measurements of GABA+ and Glx at 7T.
- Large 3D MRSI coverage with high resolution
- Robust to B0 B1+ for GABA+ and Glx editing
- 9-minute acquisition for multi-region volume quantification.
- 3D mapping of GABA+ and Glx for investigations of local and global neuropsychiatric conditions

Simultaneous Multi-Region Detection of GABA+ and Glx using 3D Spatially Resolved SLOW-editing and EPSI-readout at 7T

Guodong Weng[# 1,2], Johannes Slotboom[# 1,2], Philippe Schucht [3], Ekin Ermiş [4], Roland Wiest [1,2], Stefan Klöppel [5], Jessica Peter [5], Irena Zubak* [3] and Piotr Radojewski* [1,2]

[#] Equally contributing first authors

* Equally contributing last authors

Piotr Radojewski: piotr.radojewski@insel.ch

Guodong Weng (corresponding author): guodong.weng@unibe.ch

Affiliations:

1. Institute for Diagnostic and Interventional Neuroradiology, Inselspital, University Hospital and University of Bern, Switzerland
2. Translational Imaging Center, sitem-insel, Bern, Switzerland
3. Department of Neurosurgery, Inselspital, University Hospital and University of Bern, Switzerland
4. Department of Radiation Oncology, Inselspital, University Hospital and University of Bern, Switzerland
5. University Hospital of Old Age Psychiatry and Psychotherapy, University of Bern, Bern, Switzerland

List of abbreviations

2D: two-dimensional

3D: three-dimensional

CG: cingulate gyrus

CN: caudate nucleus

CRLB: Cramer-Rao lower bound errors

CSDA: chemical shift displacement artifact

CSI: chemical shift imaging

EPSI: echo-planar spectroscopic imaging

FID: free induction decay

FL: frontal lobe

FOV: field of view

HP: hippocampus

GABA: gamma-aminobutyric acid

GABA+: gamma-aminobutyric acid + macromolecule

Gln: glutamine

Glu: glutamate

Glx: glutamate + glutamine

GM: gray matter

MEGA: Mescher-Garwood

MIDAS: metabolic imaging data analysis system

MRI: magnetic resonance imaging

MRS: magnetic resonance spectroscopy

MRSI: magnetic resonance spectroscopic imaging

NAA: N-acetyl-aspartate

OL: occipital lobe

PET: positron emission tomography

PL: parietal lobe

PRESS: point resolved spectroscopy

PT: putamen

RF: radiofrequency

ROI: region of interest

SAR: specific absorption rate

SD: standard deviation

semiLASER/sLASER: semi localization by adiabatic selective refocusing

SLOW: Slotboom-Weng

SNR: signal-to-noise ratio

spectrIm-QMRS: spectroscopy imaging quantitative MRS(I)

SVS: single-voxel spectroscopy

TA: total acquisition

tCr: total creatine

TE: echo time

TL: thalamus

TR: repetition time

VOI: volume of interest

WM: white matter

Keywords:

GABA+, Glx, MRSI, spectral editing, SLOW, ultra-high field

Abstract

GABA+ and Glx (glutamate and glutamine) are widely studied metabolites, yet the commonly used magnetic resonance spectroscopy (MRS) techniques have significant limitations, including sensitivity to B_0 and B_1^+-inhomogeneities, limited bandwidth of MEGA-pulses, high SAR which is accentuated at 7T. To address these limitations, we propose SLOW-EPSI method, employing a large 3D MRSI coverage and achieving a high resolution down to 0.26 ml.

Simulation results demonstrate the robustness of SLOW-editing for both GABA+ and Glx against B_0 and B_1^+ inhomogeneities within the range of [-0.3, +0.3] ppm and [40%, 250%], respectively.

Two protocols, both utilizing a 70 mm thick FOV slab, were employed to target distinct brain regions *in vivo*, differentiated by their orientation: transverse and tilted. Protocol 1 (n=11) encompassed 5 locations (cortical gray matter, white matter, frontal lobe, parietal lobe, and cingulate gyrus). Protocol 2 (n=5) involved 9 locations (cortical gray matter, white matter, frontal lobe, occipital lobe, cingulate gyrus, caudate nucleus, hippocampus, putamen, and inferior thalamus).

Quantitative analysis of GABA+ and Glx was conducted in a stepwise manner. First, B_1^+/B_1–inhomogeneities were corrected using water reference data. Next, GABA+ and Glx values were calculated employing spectral fitting. Finally, the GABA+ level for each selected region was compared to the global Glx within the same subject, generating the GABA+/Glx_global ratio.

Our findings from two protocols indicate that the GABA+/Glx_global level in cortical gray matter was approximately 16% higher than in white matter. Elevated GABA+/Glx_global levels acquired with protocol 2 were observed in specific regions such as the caudate nucleus (0.118±0.067), putamen (0.108±0.023), thalamus (0.092±0.036), and occipital cortex (0.091±0.010), when compared to the cortical gray matter (0.079±0.012).

Overall, our results highlight the effectiveness of SLOW-EPSI as a robust and efficient technique for accurate measurements of GABA+ and Glx at 7T. In contrast to previous SVS and 2D-MRSI based editing sequences with which only one or a limited number of brain regions can be measured simultaneously, the method presented here measures GABA+ and Glx from any brain area and any arbitrarily shaped volume that can be flexibly selected after the examination. Quantification of GABA+ and Glx across multiple brain regions through spectral fitting is achievable with a 9-minute acquisition. Additionally, acquisition times of 18-27 minutes (GABA+) and 9-18 minutes (Glx) are required to generate 3D maps, which are constructed using Gaussian fitting and peak integration.

1. Introduction

In vivo magnetic resonance spectroscopy (MRS) and magnetic resonance spectroscopic imaging (MRSI) techniques enable non-invasive detection of multiple metabolites, such as gamma-aminobutyric acid (GABA) and glutamate in combination with glutamine (Glx). Glx refers to the sum measurement of glutamate (Glu) and glutamine (Gln). Glutamate is an excitatory neurotransmitter participating in diverse brain processes. Glx levels offer valuable insights into various neurological conditions and disorders [1]–[5]. GABA and Glx are frequently studied in conjunction [6]–[9], given their interconnected metabolism and functions. Glutamate acts as the precursor for GABA synthesis, while glutamine plays a crucial role in the glutamate-glutamine cycle, regulating the equilibrium between glutamate and GABA in the brain [10]. Additionally, the GABA/Glx ratio is often analyzed as an indicator of the balance between excitatory and inhibitory neurotransmission in the brain [9].

GABA is an important inhibitory neurotransmitter in the human central nervous system, crucial for the maintenance of brain function by balancing excitatory activity. Variations in GABA+ concentration have been extensively documented in various clinical studies, demonstrating its relevance in a number of neurological disorders. A notable example is its association with conditions characterized by altered pain perception, such as fibromyalgia and chronic pain syndromes [1]. In epilepsy, shifts in GABA concentrations have been observed after seizures [2]. The significance of GABA has been explored in diverse contexts including movement disorders [5], Alzheimer's Disease [3], insomnia [4], and various

psychiatric conditions like depression, bipolar disorder, and schizophrenia [11]–[14]. Moreover, GABA's potential utility extends to the investigation of brain tumors [15]. GABA levels in the brain are significantly lower than those of major metabolites like N-acetyl-aspartate (NAA). Moreover, the GABA spectrum has multiple resonances at chemical shifts around 1.90 ppm, 2.35 ppm, and 3.00 ppm, partially overlapping the peaks of NAA, glutamate-glutamine (Glx), and creatine (Cr). While it is possible, in principle, to separately quantify these metabolites using prior-knowledge-based quantification and non-editing localized methodologies like PRESS or semiLASER, this approach often entails reduced accuracy, indicated by substantial higher Cramér-Rao-minimum variance bound for GABA [16], [17]. Consequently, GABA measurements are seldom integrated into clinical routine due to these accuracy constraints and the lack of rapid 3D-spectroscopic imaging methodologies.

In addition to the non-editing methodologies for quantifying GABA levels in vivo, J-difference editing MRS/I techniques have emerged as primary tools for GABA detection. Non-editing approaches [18] entail fitting the spectrum using a GABA basis set [19]–[23]. Editing techniques, such as Mescher–Garwood (MEGA), often involve the co-edited detection of the macromolecular (MM) signal at 3.00 ppm, giving rise to the term GABA+ [24]–[26]. Moreover, advancements like the MM-null technique [27]–[29] for GABA-editing were introduced by placing the editing-off pulse at 1.50 ppm. These methodologies have demonstrated promise, particularly in studies with small volume-of-interest utilizing single-voxel spectroscopy (SVS) [9], [30] and single-slice MRSI [31], [32] at 3T and 7T.

A few studies have explored 3D-slab edited GABA+ in the human brain at 3T and reported challenges including low resolution (~3-4 ml) and long acquisition time (~15-20 min) [33], [34]. Moreover, achieving a large 3D volume measurements of GABA+ remains difficult, primarily due to B_0 and B_1^+ inhomogeneities, along with lipid contamination, particularly at ultra-high field strengths (≥7T) [35], [36].

A recent method described by our group specifically designed for ultra-high field strengths (SLOW-editing) [37]–[39] presents a promising novel alternative to MEGA-editing [24]. Coupled with echo-planar spectroscopic imaging (EPSI) readout [40], SLOW-editing effectively addresses several limitations associated with spectral editing in large 3D volume MRSI at ultra-high field (≥7T). These limitations include: (i) B_0- inhomogeneity; (ii) B_1^+/B_1^--inhomogeneities; (iii) limited specific absorption rate (SAR) and RF peak amplitude; (iv) chemical shift displacement artifact (CSDA) constrain; (v) signal foldback due to limited acquired spectral bandwidth; (vi) water and lipid residual signal contamination [37]A notable advantage of SLOW-editing with EPSI is its ability to *simultaneously* measure multiple neuro-anatomical regions of interest within the brain, allowing for adaptability to the shapes and sizes of the selected anatomical subregions after the examination during data analysis [37]. In contrast, MEGA-based SVS dictates a fixed location for the volume of interest, predetermined during pulse sequence planning.

Similarly, with 2D-MRSI, the choice of the spectroscopic volume of interest is constrained to anatomical regions within the same image plane.

Finally, it is crucial to emphasize that, similar to GABA+-editing with MEGA, SLOW editing also co-edits and refocuses the macromolecular signals around 3.00 ppm [37].

The goal of our study is to employ SLOW-editing technique at 7T to enable simultaneous measurement of key neuro metabolites, including GABA+ and Glx, across various brain regions. Two distinct MRSI slab (70 mm thickness) orientations (two protocols) were employed for these subjects to cover various brain regions. This approach is hypothesized to overcome limitations of current state-of-the-art methods for the measurements of GABA+ and Glx.

2. Methods

All MRI and MRSI acquisitions were performed on a Siemens 7T MR scanner (MAGNETOM Terra, Germany) in clinical mode using the standard Nova 1Tx 32Rx head coil.

2.1. Sequences

The SLOW-EPSI [37], [40] was applied in all subjects with the following parameters: TE = 68 ms, TR = 1500 ms, nominal matrix = 65 × 23 × 9, FOV = 280 × 100 × 70 mm, spatial resolution = 4.3 × 7.8 × 7.8 mm (0.26 ml), averages = 1, and TA = 9:04 min. The final matrix was interpolated into 65 × 42 ×10 (4.3 × 4.3 × 7.0 mm). The SLOW pulses serve simultaneously as *refocusing* and *editing*.

SLOW-full pulse: chemical-shift selected hyperbolic secant adiabatic pulse, 24 ms duration, 880 Hz bandwidth, 623 Hz maximum peak amplitude (corresponding to nominal flip angle 550-degree), carrier frequency at 2.9 ppm (corresponding to 1.6-4.2 ppm for passband, 4.2-4.6 ppm and 1.2-1.6 ppm for transition band).

SLOW-partial pulse: chemical-shift selected hyperbolic secant adiabatic pulse, 24 ms duration, 560 Hz bandwidth, 504 Hz maximum peak amplitude (corresponding to nominal flip angle 550-degree), carrier frequency at 3.45 ppm (corresponding to 2.7-4.2 ppm for passband, 4.2-4.6 ppm and 2.3-2.7 ppm for transition band).

2.2. Protocols and Subjects

Two protocols were performed in healthy volunteers to target distinct brain regions.

Protocol 1 used SLOW-EPSI in transverse slice orientation and was applied in 11 healthy subjects (#1-11, average age 26.7 years, 6 females and 5 males) Protocol 2 used SLOW-EPSI with slice orientation tilted along the longitudinal axis of the forebrain and was applied for comparison in 5 healthy subjects (#12-16, average age 32.4, all males)

One additional subject (#16) was measured with 4 averages SLOW-EPSI (TA = 36 minutes) of SLOW-EPSI, with the purpose of generating GABA+ and Glx maps.

2.3. Data reconstruction and pre-post-processing

For data reconstruction and pre-post-processing, the Metabolic Imaging Data Analysis System (MIDAS) [41], MATLAB R2019b, and spectrIm-QMRS[42] were used[*]. Further details are provided in the supplementary material.

2.4. Metabolite basis set simulation

The metabolite basis set for spectral fitting and quantification as well as the editing efficiency of SLOW and MEGA were simulated (**Figure 7**, **Supplementary Figure S2**, **S4**, and **S5**). The simulation of MEGA consist of excitation pulse, two non-adiabatic editing pulses (sinc-Gaussian shaped with 8.3 ms duration and a full width at half maximum (FWHM) of 128 Hz [43]), two adiabatic refocusing pulses (8 ms duration and 5 kHz bandwidth). The simulations of the spin system were performed using in-house MATLAB (R2019b) code, by solving a relaxation-free Liouville-von Neumann equation.[44]

2.5. Selection of ROIs/VOIs

ROIs/VOIs were manually selected after data acquisition in consensus of a clinical imaging expert (neuroradiologist) and a spectroscopy expert as follows:

Protocol 1: both cortical gray matter (GM) and white matter (WM), the neocortex (frontal (FL), and parietal lobe (PL)) as well as in the cingulate gyrus (CG).

Protocol 2: cortical gray matter (GM) and white matter (WM), the neocortex (frontal (FL) and occipital lobe (OL)), cingulate gyrus (CG), caudate nucleus (CN), hippocampus (HP), and putamen (PT), inferior thalamus (TL).

2.6. Water reference data acquisition

In our study, we acquired the water reference data using the same excitation pulse shape but with a smaller flip angle (10 degrees) compared to the metabolite excitation pulse (65 degrees, Ernst angle of assumed T_1 = 1700 ms) within the SLOW-EPSI sequence. [37], [40] Consequently, the B_1^-/B_1^+

[*] See: http://spectrim.diskstation.me/spectrImWeb/

inhomogeneities observed in the metabolite data are also present in the corresponding water reference data, allowing for correction. Further details are provided in the 'Discussion' section.

2.7. GABA+ and Glx values, normalization, mapping, and spectral fitting

Normalization

For each voxel (i), the spectrum S_i was normalized by the water reference signal W_i, which represents the peak integration value of water peak at voxel (i):

$$S_i = \frac{S_{raw,i}}{W_i}$$

Mapping

The normalized spectrum of subject #16 was used for mapping (**Figure 6**) using two methods: (i) Gaussian fitting and (ii) peak integration. These methods were applied to quantify GABA+ (~2.88-3.15 ppm) and Glx (~3.65-3.85 ppm). For further details, please refer to the supplementary material. It is important to note that since the spectrum was normalized by the water signal, the GABA+ and Glx mapping results are expressed in arbitrary units.

Spectral fitting

The normalized spectrum of all subjects was fitted using TDFDFit [45], which calculated the fitting area of GABA+ (3.00 ppm), denoted by A^k_{GABA+}, and Glx (3.75) ppm, denoted by A^k_{Glx}, for each selected region (k) (a sum of multiple voxels, as shown in **Figure 2** and **Figure 4**). A case of fitting line together with spectrum was shown in **Supplementary Figure S6**.

2.8. GABA+ level using global Glx as internal reference: GABA+ to Glx_global ratio

To express GABA+ levels in a meaningful unit rather than arbitrary units, we employed the mean Glx level (Glx_global) across all selected regions as the reference. The GABA+/Glx_global ratio was calculated for each selected region (k) by dividing the fitting area of GABA+, A^k_{GABA+}, in that region by the mean value of fitting area of Glx, A^k_{Glx}, across all regions.

$$\frac{GABA+(location\ k)}{Glx\_global} = \frac{A^k_{GABA}}{\sum_k A^k_{Glx}/N} \times C = \frac{A^k_{GABA}}{\bar{A}_{Glx}} \times C$$

Where A_{GABA+}^{k} is the fitting area of GABA+ at 3.00 ppm in selected region (k), $\bar{A}_{Glx}$ is the average Glx fitting area at 3.75 ppm across all regions, and N is the total number of selected regions. It is essential to note that Glx_global ($\bar{A}_{Glx}$) is a constant value within the same subject. Consequently, the GABA+/Glx_global ratio serves as an indicator of relative GABA+ levels for each selected region within the same subject.

The estimation of the GABA+/Glx_global ratio was determined by considering two factors:

(1) GABA contains two protons resonating at 3.00 ppm, while Glx has one proton at 3.75 ppm. This difference in the number of protons would result in a GABA signal twice as intense as the Glx signal if they were present in equal concentrations.
(2) The editing efficiency of GABA and Glx is slightly different, which the edited GABA signal gains more intensity (a factor of 1.2025) than Glx.

To account for these factors, a correction constant C = 2 × 1.2025 = 2.405 was introduced to quantify the GABA+/Glx_global ratio. Additional details can be found in **Supplementary Figure S2**.

2.9. Comparison with literatures which used normal GABA+/Glx ratio

In the "Discussion" section under "GABA+/Glx_global ratio," we have compiled normal GABA+/Glx ratios from published literature, where the reported ratios refer to GABA+ to Glx in specific regions or VOIs, unlike our reporting of the GABA+ to *global* Glx ratio. Our use of the GABA+/Glx_global ratio aims to capture changes in GABA+ levels *only* across various selected regions within the same subject, and is not intended to reflect the changes of *both* GABA+ and Glx levels. Consequently, Glx_global serves as a constant for each subject during the calculation of the GABA+/Glx_global ratio.

2.10. Ethics statement

All experimental protocols were approved by the local ethics committee (Ethikkommission für die Forschung am Menschen, Kantonale Ethikkommission Bern (2019-00503)). Written informed consent was obtained from all subjects.

3. Results

3.1. Protocol 1

Five anatomically distinct volumes of interest were manually selected to display the SLOW-difference spectra: The volumes and average sizes (#1-11) are shown in **Figure 2** in protocol 1: (**i.**) cortical gray matter (59.2 ml), (**ii.**) white matter (19.5 ml), (**iii.**) cingulate gyrus (4.9 ml), (**iv.**) parietal (7.3 ml) and (**v.**) frontal lobe (9.9 ml, comprising gray and white matter). The edited GABA+, Glx, and NAAG are shown at 3.00, 3.75, and 4.13 ppm, respectively (**Figure 1**). The spectra displayed in the figures show the averaged spectrum of all 11 volunteers (magenta line) with inter-individual standard deviation range (IISD (further denoted SD), indicated by gray region) .

Overall, the SD in the spectra is hardly visible, indicating the robustness of the SLOW-EPSI sequence across different individuals. However, an increased SD is observed at around 1.8 and 2.3 ppm, which can be attributed to variations in residual lipid contamination among the subjects.

The intensities of GABA+ and Glx, were lower in white matter compared to cortical gray matter. The quantifications of GABA+ and Glx in all regions were presented in the "Quantification" section below.

3.2. Protocol 2

Nine locations were manually selected in protocol 2 and the SLOW-difference spectra are displayed in **Figure 3** with corresponding average volume (#12-16) shown in **Figure 4**: cortical gray matter (37.9 ml), white matter (20.0 ml), neocortex in frontal lobe (6.9 ml), neocortex in occipital lobe (12.0 ml), cingulate gyrus (6.0 ml), hippocampus (2.5 ml), caudate nucleus (1.2 ml), putamen (2.5 ml), and thalamus (6.7 ml).

The volumes chosen for analysis exhibited a wide range varying from approximately 1.2 to 37.9 ml (**Figure 4**). Notably, the hippocampus, caudate nucleus and putamen have relatively small volume sizes, measuring 2.5 ml, 1.2 ml, and 2.5 ml, respectively. Consequently, the inter-individual standard deviation (SD) throughout their spectra (**Figure 3**) was relatively large, which can fully be attributed to the smaller volume sizes.

Examining the GABA+ intensity across the selected regions, we observed lower intensities in white matter, hippocampus, caudate nucleus, and putamen. Similarly, the Glx intensity was found to be lower in white matter, hippocampus, caudate nucleus, putamen, and thalamus. The quantifications of GABA+ and Glx in all regions were presented in the "Quantification" section.

3.3. Quantification

The quantification results of GABA+ at each selected location for all subjects are displayed in **Table 1** and **Figure 5**.

In protocol 1, the GABA+/Glx_global ratio in cortical gray matter (median value: 0.091) was 16.7% higher than in white matter (median value: 0.078). In protocol 2, the GABA+/Glx_global ratio in cortical gray matter (median value: 0.079) was 16.2% higher than in white matter (median value: 0.068). The GABA+ contrast in GW/WM was comparable in the two cohorts (**Figure 5**).

In protocol 2, the hippocampus (HP) exhibited the lowest GABA+ level (median value: 0.031), while the caudate nucleus showed the highest GABA+ level (median value: 0.118). Additionally, the putamen (PT), thalamus (TL), and neocortex (occipital lobe, OL) showed global higher GABA+ levels compared to the cortical gray matter, with values of 0.108, 0.092, and 0.091, respectively.

Table 2 shows the Cramer-Rao Lower Bound errors (CRLB) of GABA+ fitting. Overall, the majority is well below 20%, while only one case exceeds 50% which was observed in subject #15 for the caudate nucleus (CN).

3.4. Metabolite maps

The GABA+ and Glx Gaussian fitting (1 to 4 averages) and peak integration (4 averages) maps for subject #16 are displayed in **Figure 6**. The longer acquisition time results better GABA+ and Glx maps. Overall, both GABA+ and Glx exhibit a similar distribution pattern, characterized by higher levels in the gray matter and lower levels in the white matter.

3.5. Editing efficiency

Figure 7 illustrates the robust editing efficiency of the SLOW-editing within a range of [+0.4,-0.3] ppm and [40%, 250%] B_1^+ for GABA, and [+0.3,-0.4] ppm and [40%, 250%] B_1^+ for glutamate. Conversely, the editing efficiency of MEGA remains robust within a narrower range of [+0.1,-0.1] ppm and [70%, 130%] B_1^+ for GABA, and [-0.1,-0.3] ppm and [70%, 130%] B_1^+ for glutamate.

4. Discussion

4.1. Single Voxel Spectroscopy, 2D-MRSI, and 3D MRSI of the Brain

In recent years, the majority of GABA studies have utilized single voxel spectroscopy (SVS) techniques such as MEGA-PRESS [46] and MEGA-sLASER. [9], [24], [44]. Typically, these methods offer good signal-to-noise ratio (SNR) within relatively large spectroscopic volumes, typically ranging from 8 to 27 ml. However, when assessing multiple brain regions, employing multiple SVS becomes impractical due to long acquisition times. Moreover, it necessitates measuring multiple external (water) reference signals for comparison and quantification of GABA and Glx levels.

To enable the measurement of larger brain volumes, whole-slice [31] and 3D-volume [33], [34] magnetic resonance spectroscopic imaging (MRSI) techniques have been employed. Yet, traditional MEGA and chemical shift imaging (3D-CSI) sequences are time-consuming and yield low spatial resolution at clinically acceptable measurement times. It is important to note that the Gaussian modulated MEGA-pulses, which serve as non-spatial selective editing pulses rather than localization pulses, are particularly sensitive to B_0/B_1^+ inhomogeneities, which become more pronounced when larger excited/shimming volumes are examined.

In the current study, we applied the multi slice SLOW-EPSI [37] approach that effectively addresses these challenges at ultra-high field strengths (≥7T). This method does not require the separate acquisition of an internal or external water reference signal due to the fact that the EPSI [40] implementation has an integrated water reference acquisition implemented within one TR. Additionally, the method benefits from large coverage of the brain at higher spatial resolution enabling easy and robust comparisons of GABA+, Glx, and other metabolites across numerous brain regions in the same subject within one measurement. This capability to simultaneously examine multiple arbitrarily shaped parts of the brain holds promise for testing novel hypotheses within the same subjects and could advance our understanding of metabolite distributions in both normal and pathological brains.

In addition, the two protocols demonstrate the flexibility of SLOW-EPSI in measuring different combinations of brain regions based on specific study needs.

4.2. GABA+ and Glx maps

The GABA+ and Glx maps were subjected to B_1^-/B_1^+ correction using water reference data obtained during the SLOW-EPSI sequence (**Figure 6**). The B_1^- effect arises from receiver coil inhomogeneities,

while the B_1^+ effect is predominantly caused by the *non*-adiabatic excitation pulse in the presence of 1Tx transmitter coils.

To correct for these effects, we performed voxel-wise division of the metabolite data by the water reference data. It is important to acknowledge that this correction introduces variations related to water concentration and T_1 relaxation in different tissues, such as gray matter and white matter. However, due to the relatively long repetition time (TR) of 1500 ms and short echo time (TE) of ~3.5 ms or free induction decay (FID) of the water reference acquisition, the contrast arising from water concentration and T_1 relaxation in different tissues is much smaller compared to the B_1^-/B_1^+ inhomogeneities (**Supplementary Figure S3**). Thus, the utilization of water reference data for correction is justified and does not significantly bias the results.

Our results demonstrate that achieving high-quality and high-SNR 3D-maps necessitates a total acquisition (TA) time of 18-27 minutes (corresponding to 2-3 averages) for GABA+, and a TA of 9-18 minutes (1-2 averages) for Glx. In addition, the peak integration maps display analogous patterns to Gaussian fitting maps, underscoring the overall flatness of the spectral baseline across a large portion of the dataset achieved through the implementation of SLOW-EPSI, as illustrated in **Figure 6**. Notably, the Gaussian fitting maps exhibit better lateral symmetry compared to the peak integration maps, suggesting that minor baseline fluctuations can be effectively corrected using Gaussian fitting method.

The distribution patterns of GABA+ and Glx follow a similar trend, with higher concentrations in the gray matter and lower concentrations in the white matter. The only significant difference was found in slices #3 and #4, the GABA+ levels remain relatively similar to those in the gray matter, while the Glx levels are comparatively lower than in the gray matter.

It is worth noting that the maps reveal global non-uniform distribution of GABA+ and Glx levels within the gray matter (**Figure 6**). In the lower brain slices (#2, #3, and #4), both GABA+ and Glx demonstrate higher levels in the gray matter compared to the gray matter in the upper brain slices (#6, #7, and #8). Moreover, non-uniform distribution within the gray matter can also be appreciated locally within the same slices (slice #3). Consequently, estimating levels based on assumptions of uniformity and tissue segmentation [32] may introduce biases depending on the selected volume of interest.

4.3. Comparison in frontal neocortex (FL) and cingulate gyrus (CG)

Since the frontal neocortex (FL) and cingulate gyrus (CG) were measured using both protocols, we conducted a statistical comparison (t-test) of the GABA+, Glx values, and corresponding CRLB as well

as full width at half maximum (FWHM) to determine if there were statistically significant differences between the two protocols.

Frontal neocortex (FL)

The water-reference-corrected GABA+ (*protocol #1*: mean ± SD = 5.07±1.57, *protocol #2*: mean ± SD = 6.03±2.16; p = 0.3288) and Glx (*protocol #1*: mean ± SD = 30.57±5.21, *protocol #2*: mean ± SD = 31.5±7.07; p = 0.7728) values in arbitrary unit exhibited no statistical differences between the two protocols. Similarly, the CRLB and FWHM demonstrated no statistical differences between two protocols: CRLB for GABA+ (*protocol #1*: mean ± SD = 10.64±5.15%, *protocol #2*: mean ± SD = 10.96±4.19%; p = 0.9046) and Glx (*protocol #1*: mean ± SD = 5.34±2.14%, *protocol #2*: mean ± SD = 6.05±2.49%; p = 0.5666); FWHM for GABA+ (*protocol #1*: mean ± SD = 33.45±5.87 Hz, *protocol #2*: mean ± SD = 33.40±8.50 Hz; p = 0.9882) and Glx (*protocol #1*: mean ± SD = 20.18±1.60 Hz, *protocol #2*: mean ± SD = 20.80±2.49 Hz; p = 0.5556).

Cingulate gyrus (CG)

the water-reference-corrected GABA+ value in arbitrary unit exhibited a statistical difference between the two protocols (*protocol #1*: mean ± SD = 8.12±5.21, *protocol #2*: mean ± SD =4.37±7.07; p = 0.0411), while Glx showed no statistical differences (*protocol #1*: mean ± SD = 31.40±5.21, *protocol #2*: mean ± SD =28.54±7.07; p = 0.4799). The CRLB and FWHM also demonstrated no statistical differences between the protocols: CRLB for GABA+ (*protocol #1*: mean ± SD = 9.66±4.09%, *protocol #2*: mean ± SD = 10.33±2.72%; p = 0.7487) and Glx (*protocol #1*: mean ± SD = 6.68±2.45%, *protocol #2*: mean ± SD = 4.77±1.01%; p = 0.1212); FWHM for GABA+ (*protocol #1*: mean ± SD = 26.90±11.55 Hz, *protocol #2*: mean ± SD = 33.60±8.71 Hz; p = 0.2760) and Glx (*protocol #1*: mean ± SD = 20.30±2.00 Hz, *protocol #2*: mean ± SD = 19.80±0.84 Hz; p = 0.6066).

The consistent FWHM values across both protocols indicate that B_0 shimming does not significantly impact the two regions due to the different orientations. Similarly, the lack of significant differences in CRLB suggests that spectral quality remains unaffected by the two different orientations. However, the GABA+ values at cingulate gyrus exhibit a significant difference between the two protocols, while Glx does not. Since the two protocols examined different subjects, it is not possible to definitively conclude that the different orientations of the two protocols significantly alter the measured GABA+ and Glx values or that this is due to physiological differences. Further investigation is required to address this issue, but it lies beyond the scope of the current study. It is crucial to emphasize that the primary objective of this study lies in demonstrating the feasibility and applicability of both SLOW-EPSI protocols for measuring GABA+ and Glx in multiple brain regions at 7T. The determination of the optimal SLOW-

EPSI protocol is not within the scope of this study, as the regions of interest for measurement may vary depending on specific research objectives.

4.4. GABA+/Glx_global ratio

Previous studies have shown a variable GABA+/Glx ratios of approximately 0.15-0.2 (Spurny et al.[6]), 0.2-0.3 (Tapper et al.[7]), 0.3-0.4 (Zhang et al.[8]) at 3T, and 0.07-0.09 (Finkelman et al.[9]) at 7T. Our result shows the *mean* ± *SD* GABA+/Glx ratio for protocol 1 (0.0902±0.0287) and protocol 2 (0.0865±0.0373), which is consistent with the study by Finkelman *et al*. [9] at 7T. It is crucial to note that these ratios represent GABA+ to Glx levels within each selected VOI or region, differing from the GABA+ to Glx_global ratio in this study.

To assess the GABA+ levels across different brain regions, Glx_global was used as an internal reference instead of Glx within each region in our study. In previous studies GABA+/tCr (total creatine) ratio has commonly been used with tCr is fitted with full spectra (MEGA-off) [6], [47]. This approach requires precise fitting due to the presence of various metabolites resonating around 3.20 ppm. These overlapping metabolites, such as glucose, glycine, myo-inositol, phenylalanine, phosphoethanolamine, taurine, and homocarnosine, make accurate fitting challenging. In contrast, although the signal-to-noise ratio (SNR) of Glx in the editing-difference spectra is lower compared to tCr in the full spectra, the presence of overlapping metabolites is significantly reduced. Moreover, MEGA-editing is more susceptible to B_0/B_1^+ inhomogeneities, with the carrier center typically placed at 1.90 ppm, which is optimal for GABA editing (J-coupled spins at about 1.90 ppm) but not for co-edited Glx (J-coupled spins at about 2.12 ppm). Therefore, Glx is even more sensitive to B_0/B_1^+ inhomogeneities when using MEGA (**Figure 7** and **Supplementary Figure S4-S5**) compared to SLOW. In contrast, simulation results demonstrate the robustness of SLOW-editing for both GABA and Glx (using Glu as an example) within the range of [+0.3, -0.3] ppm ΔB_0 and [40%, 250%] B_1^+, making Glx a suitable internal reference metabolite (**Figure 7** and **Supplementary Figure S4-S5**).

4.5. Limitations

One limitation of the SLOW-EPSI technique employed in our study is the restricted coverage of the field of view (FOV), which has a height of 70 mm. Consequently, not all the regions of interest, such as both the neocortex (parietal) and hippocampus, were fully measured within the FOV. To address this limitation, one potential solution could be to increase the FOV height to 100-120 mm and adjust the phase-encoding steps from approximately 9 to 13-15 while maintaining at least a similar resolution. It is worth noting that

further reduction of the TR is feasible as SLOW-EPSI is a low specific absorption rate (SAR) technique compared to sLASER and the described protocols are not running at maximum (clinically) allowed SAR. Therefore, the low SAR of the method allows for additional flexibility to further optimize several acquisition parameters, such as shorter TR.

To achieve GABA+ and Glx maps, we opted for Gaussian fitting and peak integration (see **Supplementary Figure S1**) instead of prior knowledge based spectral fitting using Voigt lines due to the considerable time requirements of current fitting algorithms. The 3D-resolved SLOW-EPSI MRSI dataset comprises a maximum of 27,300 voxels (including non-brain voxels), making robust spectral fitting challenging but also very time consuming. Currently efforts are made in our institute to speed up the time needed to do fitting [48]. It could be shown by using a classical fitting approach using Pytorch, that an increase of a factor 12 in computation speed could easily be achieved. Currently, even much higher acceleration factors seem possible and will show elsewhere soon. However, leveraging a fast spectral fitting algorithm utilizing machine learning, would greatly enhance the analysis process given the large voxel count [49].

The quantification of GABA+ and Glx levels using spectral fitting did not include T_1 and T_2 relaxation correction for different tissue types. Currently, the assumption of uniform T_1 and T_2 values within the same tissue is commonly employed, which is reasonable for small volume studies using single voxel spectroscopy (SVS). However, this assumption becomes less robust when considering whole-brain coverage, and brain lesions. In future studies, the inclusion of corresponding T_2 maps, especially for GABA+ quantification is expected to address this limitation. By incorporating T_2 relaxation correction, more accurate and tissue-specific measurements of GABA+ and Glx levels can be obtained, enhancing the reliability and interpretation of the results.

The SLOW-editing technique was initially developed for ultra-high field scanners (≥7T) due to the scaling of chemical shift with B_0, which facilitates effective chemical-shift selectivity using SLOW pulses. This approach demonstrates exceptional performance in terms of B_0 robustness and water/lipid suppression. However, the widespread availability and utilization of 7T scanners remain limited, restricting the application of SLOW editing. To address this challenge, a 3T version of SLOW is under development, and promising preliminary results have been obtained at our institution. The 3T version of SLOW is anticipated to be available in the near future.

5. Conclusion

The presented SLOW-editing for simultaneous detection of neurotransmitters - GABA+ and Glx - is not only feasible but also robust when comparing results across different individuals. Notably, a 9-minute acquisition allows for quantification of GABA+ and Glx across multiple anatomical regions in brain. The two protocols demonstrate the flexibility of SLOW-EPSI in measuring and analyzing distinct sets of brain regions based on specific study requirements. Generating comprehensive 3D maps for GABA+ and Glx necessitates acquisition times of 18-27 minutes and 9-18 minutes, respectively. This sequence holds substantial promise for both neuroscience research and clinical applications, particularly in investigating alterations in neurotransmitter levels in both focal and global neurological conditions.

CRediT authorship contribution statement

Ethics committee approval (JS). Study design and preparation (JS, RW, PR). MRSI methodology (GW, JS). Volunteer recruitment (PS, EE, RW, SK, JP, IZ). Data analysis (GW, JS, PR). Manuscript preparation (GW, JS, PR). Manuscript editing (all authors).

Declaration of Competing Interest

Guodong Weng and Johannes Slotboom disclose that the application of SLOW-editing described in the paper has been filed at the International Bureau of WIPO as a PCT patent application.

Patent applicant: Universität Bern.

Status of application: published (WO 2022/229728).

Inventors: Guodong Weng and Johannes Slotboom

Data availability

Data will be made available on request.

Acknowledgement

The funding was provided by Schweizerischer Nationalfonds zur Förderung der Wissenschaftlichen Forschung, SNSF-182569.

Reference

[1] A. L. Peek, T. Rebbeck, N. AJ. Puts, J. Watson, M.-E. R. Aguila, and A. M. Leaver, "Brain GABA and glutamate levels across pain conditions: A systematic literature review and meta-analysis of 1H-MRS studies using the MRS-Q quality assessment tool," *Neuroimage*, vol. 210, p. 116532, Apr. 2020, doi: 10.1016/j.neuroimage.2020.116532.

[2] G. L. Sarlo and K. F. Holton, "Brain concentrations of glutamate and GABA in human epilepsy: A review," *Seizure*, vol. 91, pp. 213–227, Oct. 2021, doi: 10.1016/j.seizure.2021.06.028.

[3] M. Solas, E. Puerta, and M. Ramirez, "Treatment Options in Alzheimer´s Disease: The GABA Story," *Curr Pharm Des*, vol. 21, no. 34, pp. 4960–4971, Oct. 2015, doi: 10.2174/1381612821666150914121149.

[4] D. T. Plante, J. E. Jensen, and J. W. Winkelman, "The Role of GABA in Primary Insomnia," *Sleep*, vol. 35, no. 6, pp. 741–742, Jun. 2012, doi: 10.5665/sleep.1854.

[5] H. Boecker, "Imaging the Role of GABA in Movement Disorders," *Curr Neurol Neurosci Rep*, vol. 13, no. 10, p. 385, Oct. 2013, doi: 10.1007/s11910-013-0385-9.

[6] B. Spurny-Dworak *et al.*, "The influence of season on glutamate and <scp>GABA</scp> levels in the healthy human brain investigated by magnetic resonance spectroscopy imaging," *Hum Brain Mapp*, vol. 44, no. 6, pp. 2654–2663, Apr. 2023, doi: 10.1002/hbm.26236.

[7] S. Tapper, N. Göransson, P. Lundberg, A. Tisell, and P. Zsigmond, "A pilot study of essential tremor: cerebellar GABA+/Glx ratio is correlated with tremor severity," *Cerebellum Ataxias*, vol. 7, no. 1, p. 8, Dec. 2020, doi: 10.1186/s40673-020-00116-y.

[8] L. Zhang *et al.*, "Symptom improvement in children with autism spectrum disorder following bumetanide administration is associated with decreased GABA/glutamate ratios," *Transl Psychiatry*, vol. 10, no. 1, p. 9, Jan. 2020, doi: 10.1038/s41398-020-0692-2.

[9] T. Finkelman, E. Furman-Haran, R. Paz, and A. Tal, "Quantifying the excitatory-inhibitory balance: A comparison of SemiLASER and MEGA-SemiLASER for simultaneously measuring GABA and glutamate at 7T," *Neuroimage*, vol. 247, p. 118810, Feb. 2022, doi: 10.1016/J.NEUROIMAGE.2021.118810.

[10] L. K. Bak, A. Schousboe, and H. S. Waagepetersen, "The glutamate/GABA-glutamine cycle: aspects of transport, neurotransmitter homeostasis and ammonia transfer," *J Neurochem*, vol. 98, no. 3, pp. 641–653, Aug. 2006, doi: 10.1111/j.1471-4159.2006.03913.x.

[11] C. G. Ting Wong, T. Bottiglieri, and O. C. Snead, "GABA, ?-hydroxybutyric acid, and neurological disease," *Ann Neurol*, vol. 54, no. S6, pp. S3–S12, 2003, doi: 10.1002/ana.10696.

[12] B. Sun *et al.*, "Imbalance between GABAergic and Glutamatergic Transmission Impairs Adult Neurogenesis in an Animal Model of Alzheimer's Disease," *Cell Stem Cell*, vol. 5, no. 6, pp. 624–633, Dec. 2009, doi: 10.1016/j.stem.2009.10.003.

[13] P. K. Mandal, K. Kansara, and A. Dabas, "The GABA–Working Memory Relationship in Alzheimer's Disease," *J Alzheimers Dis Rep*, vol. 1, no. 1, pp. 43–45, Jul. 2017, doi: 10.3233/ADR-170003.

[14] C. Chiapponi, F. Piras, F. Piras, C. Caltagirone, and G. Spalletta, "GABA System in Schizophrenia and Mood Disorders: A Mini Review on Third-Generation Imaging Studies," *Front Psychiatry*, vol. 7, Apr. 2016, doi: 10.3389/fpsyt.2016.00061.

[15] P. Sharma, A. Aaroe, J. Liang, and V. K. Puduvalli, "Tumor microenvironment in glioblastoma: Current and emerging concepts," *Neurooncol Adv*, vol. 5, no. 1, pp. 1–16, Jan. 2023, doi: 10.1093/NOAJNL/VDAD009.

[16] M. Považan *et al.*, "Comparison of Multivendor Single-Voxel MR Spectroscopy Data Acquired in Healthy Brain at 26 Sites," *Radiology*, vol. 295, no. 1, pp. 171–180, Apr. 2020, doi: 10.1148/radiol.2020191037.

[17] J. Near *et al.*, "Preprocessing, analysis and quantification in single-voxel magnetic resonance spectroscopy: experts' consensus recommendations," *NMR Biomed*, vol. 34, no. 5, p. e4257, May 2021, doi: 10.1002/NBM.4257.

[18] S. W. Provencher, "Estimation of metabolite concentrations from localizedin vivo proton NMR spectra," *Magn Reson Med*, vol. 30, no. 6, Dec. 1993, doi: 10.1002/mrm.1910300604.

[19] R. Mekle, V. Mlynárik, G. Gambarota, M. Hergt, G. Krueger, and R. Gruetter, "MR spectroscopy of the human brain with enhanced signal intensity at ultrashort echo times on a clinical platform at 3T and 7T," *Magn Reson Med*, vol. 61, no. 6, pp. 1279–1285, Jun. 2009, doi: 10.1002/MRM.21961.

[20] A. Napolitano, W. Kockenberger, and D. P. Auer, "Reliable gamma aminobutyric acid measurement using optimized PRESS at 3 T," *Magn Reson Med*, vol. 69, no. 6, pp. 1528–1533, Jun. 2013, doi: 10.1002/mrm.24397.

[21] I. Tkáč, G. Öz, G. Adriany, K. Uğurbil, and R. Gruetter, "In vivo ^{1}H NMR spectroscopy of the human brain at high magnetic fields: Metabolite quantification at 4T vs. 7T," *Magn Reson Med*, vol. 62, no. 4, pp. 868–879, Oct. 2009, doi: 10.1002/mrm.22086.

[22] T. Okada *et al.*, "Repeatability of proton magnetic resonance spectroscopy of the brain at 7 T: effect of scan time on semi-localized by adiabatic selective refocusing and short-echo time stimulated echo acquisition mode scans and their comparison," *Quant Imaging Med Surg*, vol. 11, no. 1, pp. 9–20, Jan. 2021, doi: 10.21037/qims-20-517.

[23] S. Younis *et al.*, "Feasibility of Glutamate and GABA Detection in Pons and Thalamus at 3T and 7T by Proton Magnetic Resonance Spectroscopy," *Front Neurosci*, vol. 14, Oct. 2020, doi: 10.3389/fnins.2020.559314.

[24] M. Mescher, H. Merkle, J. Kirsch, M. Garwood, and R. Gruetter, "Simultaneous in vivo spectral editing and water suppression," *NMR Biomed*, vol. 11, no. 6, pp. 266–272, Oct. 1998, doi: 10.1002/(SICI)1099-1492(199810)11:6<266::AID-NBM530>3.0.CO;2-J.

[25] R. A. E. Edden and P. B. Barker, "Spatial effects in the detection of γ-aminobutyric acid: Improved sensitivity at high fields using inner volume saturation," *Magn Reson Med*, vol. 58, no. 6, pp. 1276–1282, Dec. 2007, doi: 10.1002/mrm.21383.

[26] K. W. Waddell, M. J. Avison, J. M. Joers, and J. C. Gore, "A practical guide to robust detection of GABA in human brain by J-difference spectroscopy at 3 T using a standard volume coil," *Magn Reson Imaging*, vol. 25, no. 7, pp. 1032–1038, Sep. 2007, doi: 10.1016/j.mri.2006.11.026.

[27] A. D. Harris, N. A. J. Puts, P. B. Barker, and R. A. E. Edden, "Spectral-editing measurements of GABA in the human brain with and without macromolecule suppression," *Magn Reson Med*, vol. 74, no. 6, pp. 1523–1529, Dec. 2015, doi: 10.1002/mrm.25549.

[28] R. A. E. Edden, N. A. J. Puts, and P. B. Barker, "Macromolecule-suppressed GABA-edited magnetic resonance spectroscopy at 3T," *Magn Reson Med*, vol. 68, no. 3, pp. 657–661, Sep. 2012, doi: 10.1002/mrm.24391.

[29] R. A. E. Edden *et al.*, "Prospective frequency correction for macromolecule-suppressed GABA editing at 3T," *Journal of Magnetic Resonance Imaging*, vol. 44, no. 6, pp. 1474–1482, Dec. 2016, doi: 10.1002/jmri.25304.

[30] D. Hong, S. Rohani Rankouhi, J.-W. Thielen, J. J. A. van Asten, and D. G. Norris, "A comparison of sLASER and MEGA-sLASER using simultaneous interleaved acquisition for measuring GABA in the human brain at 7T," *PLoS One*, vol. 14, no. 10, p. e0223702, Oct. 2019, doi: 10.1371/journal.pone.0223702.

[31] P. Moser *et al.*, "Whole-slice mapping of GABA and GABA+ at 7T via adiabatic MEGA-editing, real-time instability correction, and concentric circle readout," *Neuroimage*, vol. 184, pp. 475–489, Jan. 2019, doi: 10.1016/j.neuroimage.2018.09.039.

[32] J. E. Jensen, B. de B. Frederick, and P. F. Renshaw, "Grey and white matter GABA level differences in the human brain using two-dimensional, J-resolved spectroscopic imaging," *NMR Biomed*, vol. 18, no. 8, pp. 570–576, Dec. 2005, doi: 10.1002/NBM.994.

[33] R. E. Ma, J. B. Murdoch, W. Bogner, O. Andronesi, and U. Dydak, "Atlas-based GABA mapping with 3D MEGA-MRSI: Cross-correlation to single-voxel MRS," *NMR Biomed*, vol. 34, no. 5, May 2021, doi: 10.1002/nbm.4275.

[34] B. Spurny *et al.*, "Automated ROI-Based Labeling for Multi-Voxel Magnetic Resonance Spectroscopy Data Using FreeSurfer," *Front Mol Neurosci*, vol. 12, Feb. 2019, doi: 10.3389/fnmol.2019.00028.

[35] M. A. Dieringer *et al.*, "Rapid Parametric Mapping of the Longitudinal Relaxation Time T1 Using Two-Dimensional Variable Flip Angle Magnetic Resonance Imaging at 1.5 Tesla, 3 Tesla, and 7 Tesla," *PLoS One*, vol. 9, no. 3, p. e91318, Mar. 2014, doi: 10.1371/JOURNAL.PONE.0091318.

[36] J. P. Stockmann and L. L. Wald, "In vivo B0 field shimming methods for MRI at 7 T," *Neuroimage*, vol. 168, pp. 71–87, Mar. 2018, doi: 10.1016/J.NEUROIMAGE.2017.06.013.

[37] G. Weng *et al.*, "SLOW: A novel spectral editing method for whole-brain MRSI at ultra high magnetic field," *Magn Reson Med*, vol. 88, no. 1, pp. 53–70, Jul. 2022, doi: 10.1002/mrm.29220.

[38] G. Weng *et al.*, "Accurate prediction of isocitrate dehydrogenase -mutation status of gliomas using SLOW-editing magnetic resonance spectroscopic imaging at 7 T MR," *Neurooncol Adv*, vol. 5, no. 1, pp. 1–14, Jan. 2023, doi: 10.1093/NOAJNL/VDAD001.

[39] G. Weng, P. Radojewski, and J. Slotboom, "α-D-Glucose as a non-radioactive MRS tracer for metabolic studies of the brain," *Sci Rep*, vol. 13, no. 1, p. 6159, Apr. 2023, doi: 10.1038/s41598-023-33161-8.

[40] A. Ebel and A. A. Maudsley, "Improved spectral quality for 3D MR spectroscopic imaging using a high spatial resolution acquisition strategy," *Magn Reson Imaging*, vol. 21, no. 2, pp. 113–120, 2003, doi: 10.1016/S0730-725X(02)00645-8.

[41] A. A. Maudsley *et al.*, "Comprehensive processing, display and analysis forin vivo MR spectroscopic imaging," *NMR Biomed*, vol. 19, no. 4, pp. 492–503, Jun. 2006, doi: 10.1002/nbm.1025.

[42] N. Pedrosa de Barros, R. Mckinley, U. Knecht, R. Wiest, and J. Slotboom, "Automatic quality control in clinical 1H MRSI of brain cancer," *NMR Biomed*, vol. 29, no. 5, pp. 563–575, May 2016, doi: 10.1002/NBM.3470.

[43] C. Chen *et al.*, "Activation induced changes in GABA: Functional MRS at 7 T with MEGA-sLASER," *Neuroimage*, vol. 156, pp. 207–213, Aug. 2017, doi: 10.1016/j.neuroimage.2017.05.044.

[44] J. Slotboom, A. F. Mehlkopf, and W. M. M. J. Bovee, "The Effects of Frequency-Selective RF Pulses on J-Coupled Spin-1/2 Systems," *J Magn Reson A*, vol. 108, no. 1, pp. 38–50, May 1994, doi: 10.1006/JMRA.1994.1086.

[45] J. Slotboom, C. Boesch, and R. Kreis, "Versatile frequency domain fitting using time domain models and prior knowledge," *Magn Reson Med*, vol. 39, no. 6, pp. 899–911, Jun. 1998, doi: 10.1002/mrm.1910390607.

[46] J. M. Duda *et al.*, "Repeatability and reliability of GABA measurements with magnetic resonance spectroscopy in healthy young adults," *Magn Reson Med*, vol. 85, no. 5, pp. 2359–2369, May 2021, doi: 10.1002/mrm.28587.

[47] S. I. Lim and L. Xin, "γ-aminobutyric acid measurement in the human brain at 7 T: Short echo-time or Mescher–Garwood editing," *NMR Biomed*, vol. 35, no. 7, p. e4706, Jul. 2022, doi: 10.1002/NBM.4706.

[48] F. Turco and J. Slotboom, “Prior-knowledge MRS Metabolite Quantification using Deep Learning Frameworks: A proof-of-concept,” in *ISMRM & SMRT Annual Meeting & Exhibition*, London, May 2022, p. 2523.

[49] R. Rizzo, M. Dziadosz, S. P. Kyathanahally, A. Shamaei, and R. Kreis, “Quantification of MR spectra by deep learning in an idealized setting: Investigation of forms of input, network architectures, optimization by ensembles of networks, and training bias,” *Magn Reson Med*, vol. 89, no. 5, pp. 1707–1727, May 2023, doi: 10.1002/mrm.29561.

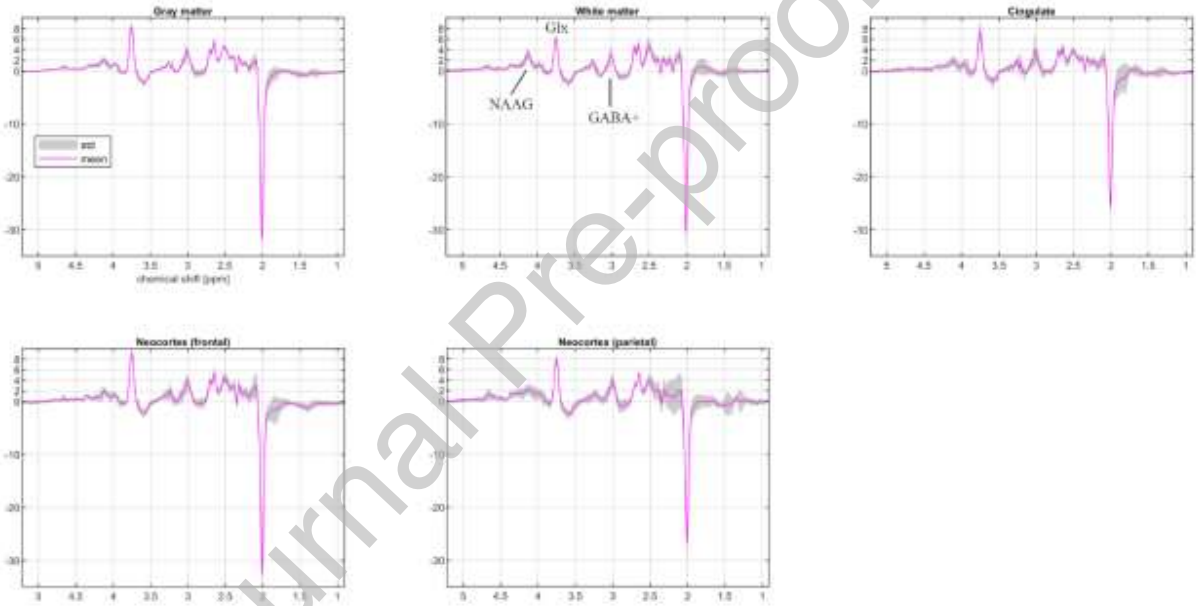

Figure 1: Editing spectra of SLOW-EPSI in 11 heathy volunteers (#1-11). The magenta line is the average spectrum of 11 subjects at different locations. The gray area is the standard deviation of the spectra of 11 subjects. The corresponding selected locations are shown in **Figure 2**

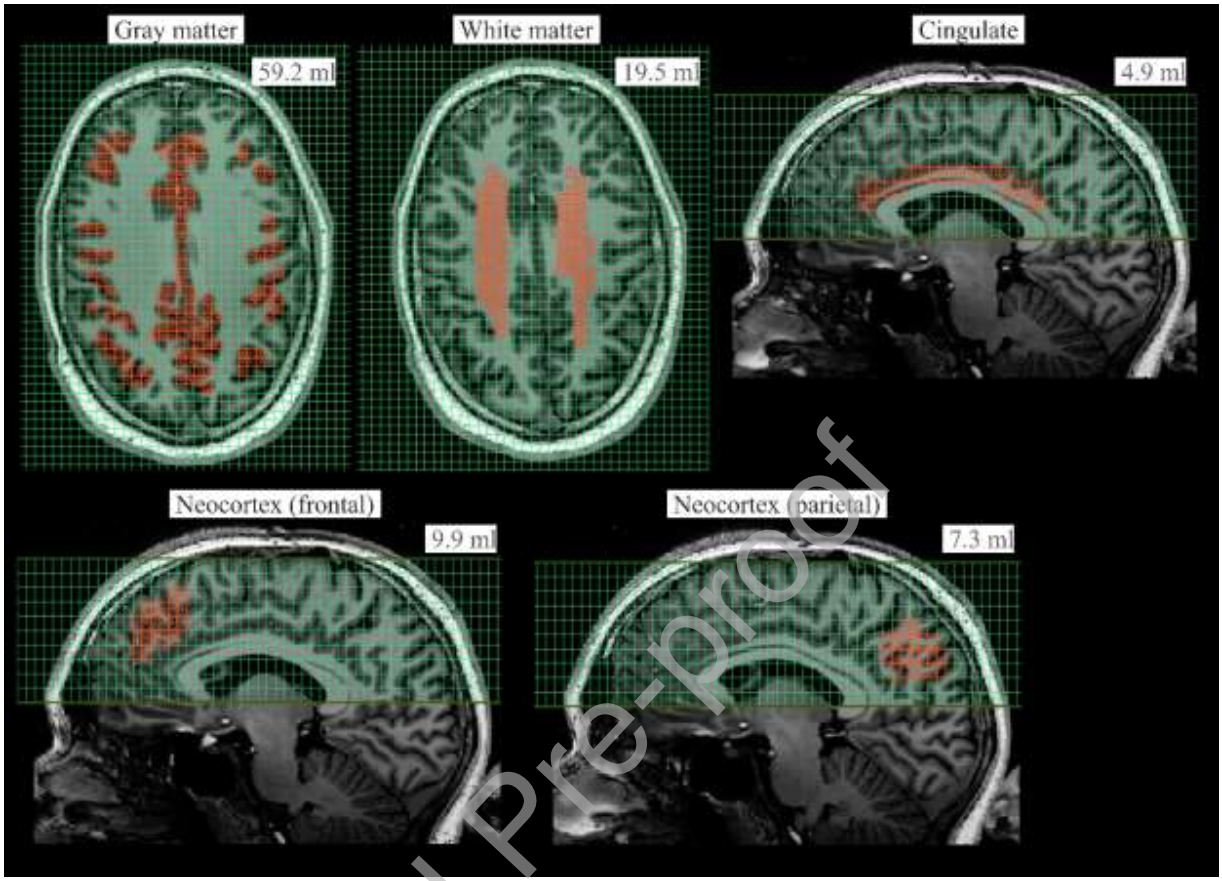

Figure 2: T1-weighted MRI and the selected regions corresponding to **Figure 1** of one subject (#11). The size of the selected VOIs is indicated for each location. Note that for simplicity only one slice has been shown and the selected VOIs cover 2-4 slices, and the volume sizes shown are the average values of 11 subjects (#1-11).

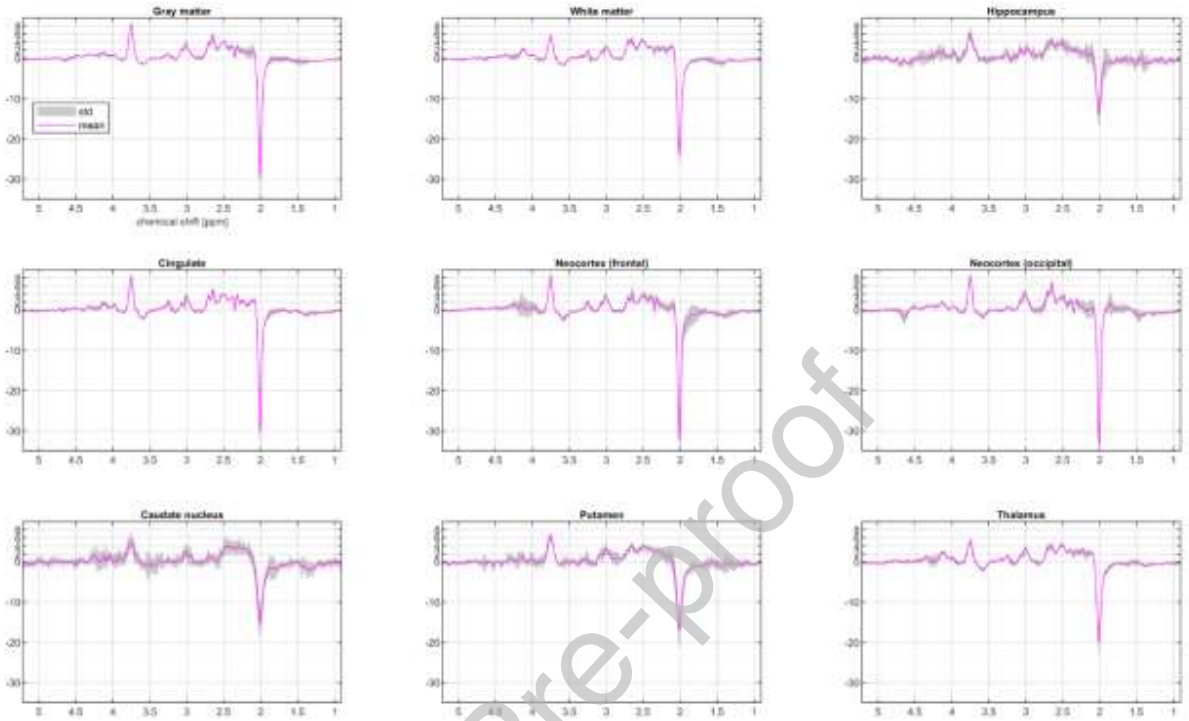

Figure 3: Editing spectra of SLOW-EPSI in 5 heathy volunteers (#12-16). The magenta line is the average spectrum of 5 subjects at different locations. The gray area is the standard deviation of the spectra of 5 subjects. The corresponding selected locations are shown in **Figure 4**

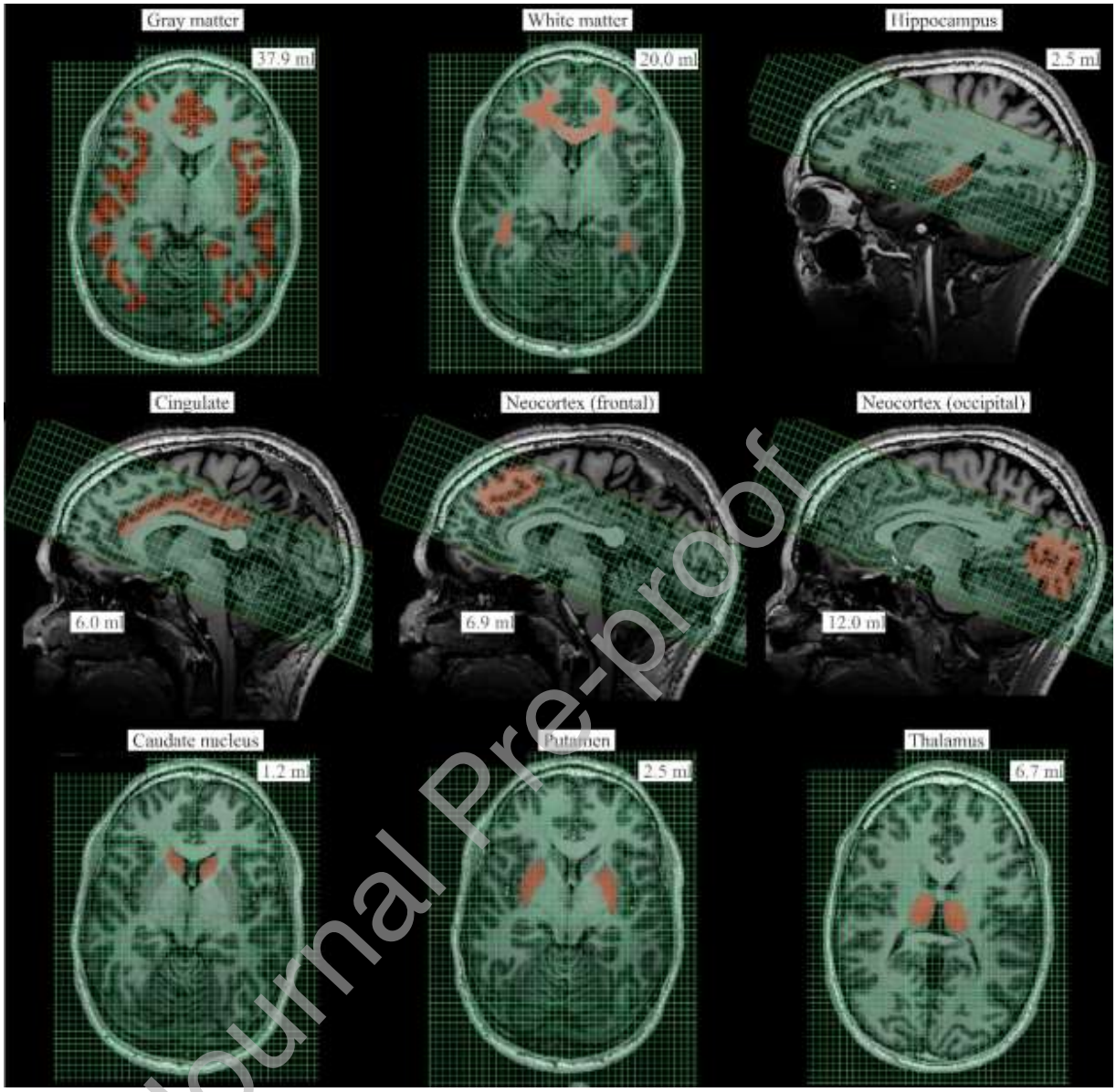

Figure 4: T1-weighted MRI and the selected regions corresponding to **Figure 3** of one subject (#16). The size of the selected VOIs is indicated for each location. Note that for simplicity only one slice has been shown and the selected VOIs cover 2-4 slices, and the volume sizes shown are the average values of 5 subjects (#12-16).

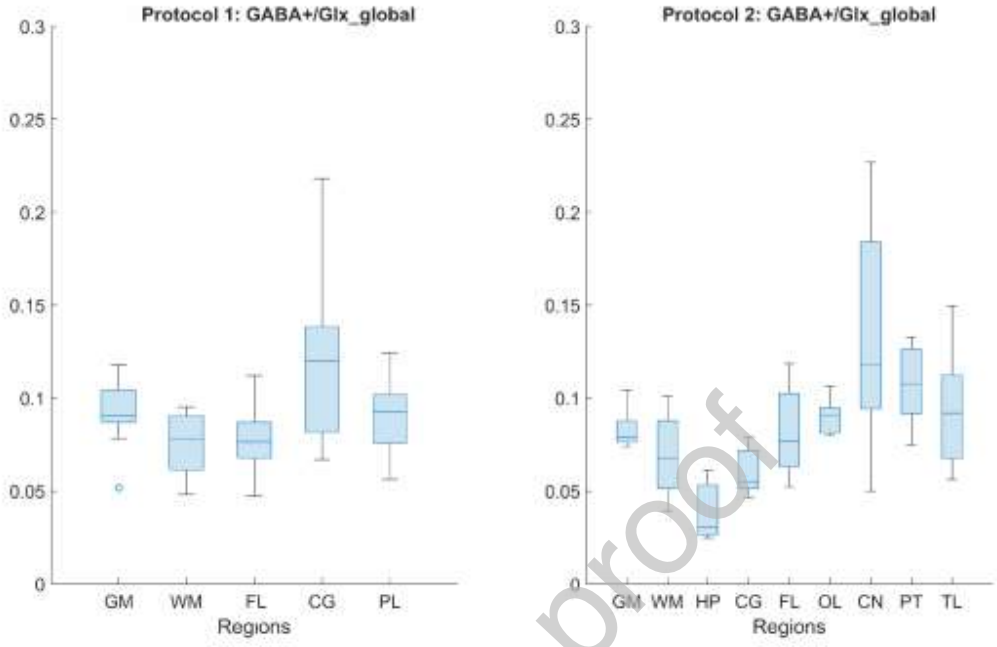

Figure 5: Box and whiskers plot of GABA+/Glx_global ratio for all subjects.

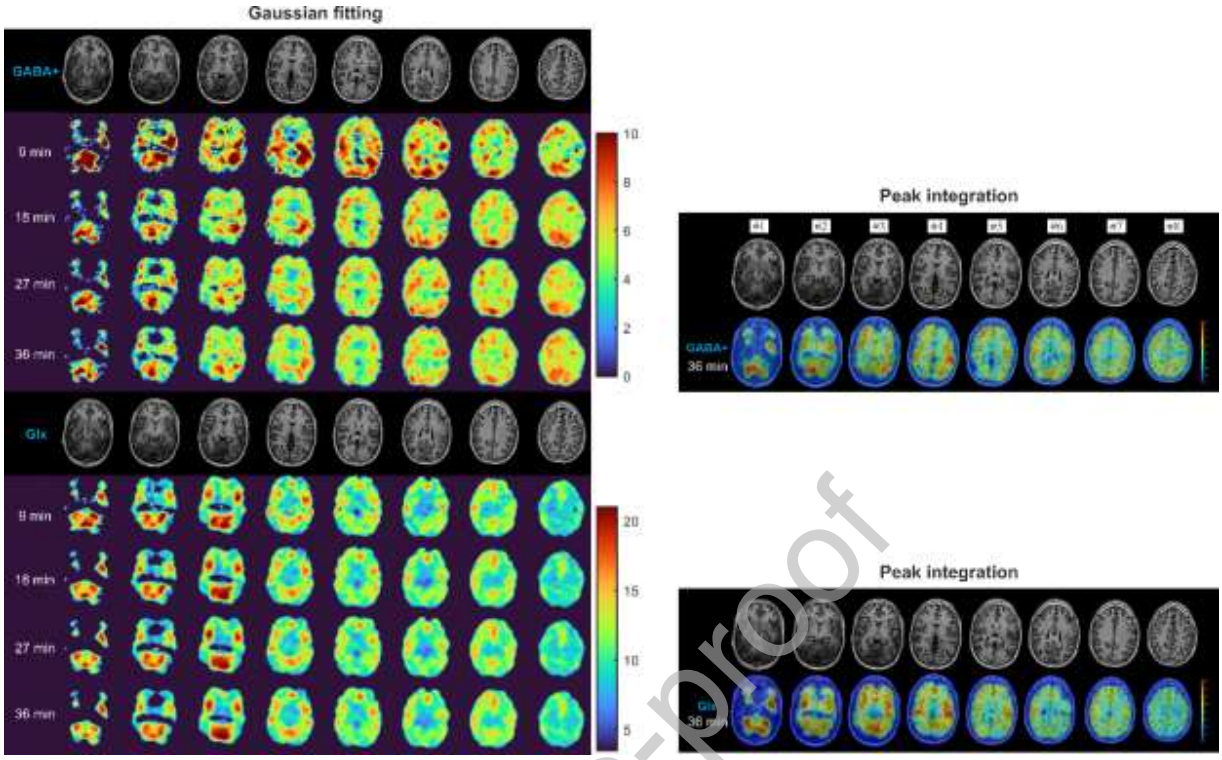

Figure 6: GABA+ and Glx maps the subject (#16) in arbitrary unit. **Left)** Gaussian fitting maps with different acquisition time (9-36 minutes). **Right)** Peak integration maps with 36 minutes acquisition.

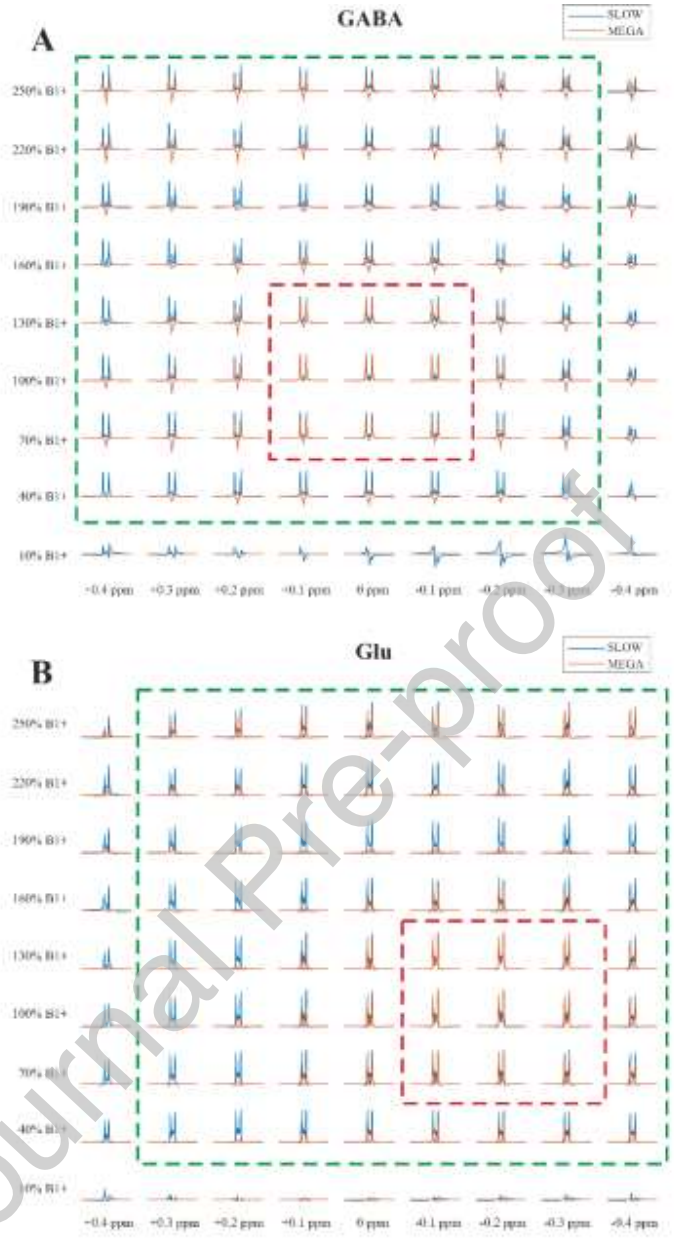

Figure 7: **Simulation of GABA and glutamate editing performance with SLOW vs MEGA as a function of B_0 and B_1^+.** The MEGA-pulses were sinc-Gaussian shaped with 8.3 ms duration and a full width at half maximum (FWHM) of 128 Hz, functioning as editing pulses but not localization pulses [43]. **A)** The SLOW-editing (blue) for GABA is robust within [+0.4,-0.3] ppm and [40%, 250%] B_1^+ (indicated by green rectangle) compared to MEGA (orange) within [+0.1,-0.1] ppm ΔB_0 and [70%, 130%] B_1^+ (indicated by red rectangle). **B)** The SLOW-editing (blue) for glutamate is robust within [+0.3,-0.4] ppm and [40%, 250%] B_1^+ (indicated by green rectangle) compared to MEGA (orange) within [-0.1,-0.3] ppm ΔB_0 and [70%, 130%] B_1^+ (indicated by red rectangle).

Table 1: GABA+/Glx_global ratio for all subjects. '-' means not detected.

Subject	Gender	Age	Cortical gray matter	White matter	Parietal lobe	Cingulate gyrus	Frontal lobe	Hippocampus	Occipital lobe	Caudate nucleus	Putamen	Thalamus
1	M	26	0.078	0.093	0.124	0.143	0.067					
2	M	27	0.106	0.095	0.104	0.067	0.070					
3	M	29	0.105	0.078	0.061	0.138	0.112					
4	F	29	0.090	0.078	0.056	0.080	0.084					
5	F	21	0.100	0.087	0.073	0.130	0.071					
6	M	22	0.095	0.078	0.109	0.109	0.081					
7	F	29	0.086	0.059	0.086	0.137	0.088					
8	F	27	0.052	0.048	0.095	-	0.103					
9	F	26	0.118	0.091	0.092	0.218	0.047					
10	F	30	0.091	0.066	0.094	0.082	0.076					
11	M	28	0.090	0.060	0.083	0.097	0.052					
Median (#1-11)			**0.091± 0.017**	**0.078± 0.016**	**0.092± 0.020**	**0.120± 0.044**	**0.076± 0.020**					
12	M	36	0.082	0.068		0.055	0.066	-	0.091	0.050	0.133	0.100
13	M	33	0.074	0.039		0.052	0.118	-	0.080	0.109	0.124	0.056
14	M	33	0.104	0.101		0.069	0.052	0.031	0.106	0.227	0.108	0.150
15	M	29	0.077	0.055		0.047	0.097	0.061	0.091	0.169	0.075	0.071
16	M	31	0.079	0.083		0.079	0.077	0.025	0.082	0.118	0.097	0.092
Median (#12-16)			**0.079± 0.012**	**0.068± 0.024**		**0.055± 0.013**	**0.077± 0.026**	**0.031± 0.019**	**0.091± 0.010**	**0.118± 0.067**	**0.108± 0.023**	**0.092± 0.036**

Table 2: Cramer-Rao Lower Bound (CRLB) of GABA+ fitting. '-' means not detected. The row below each CRLB value shows the volume size of the selected region.

Subject	Gender	Age	Cortical gray matter [%]	White matter [%]	Parietal lobe [%]	Cingulate [%]	Frontal lobe [%]	Hippocampus [%]	Occipital lobe [%]	Caudate nucleus [%]	Putamen [%]	Thalamus [%]
1	M	26	**6.81**	**6.53**	**8.77**	**6.17**	**8.13**					
			66.4	32.8	11.3	4.9 ml	8.2					
2	M	27	**6.84**	**13.7**	**13.26**	**19.09**	**9.76**					
			58.8	23.5	5.1	4.0 ml	7.0					
3	M	29	**9.06**	**13.7**	**17.84**	**10.07**	**16.60**					
			71.1	20.3	6.5	3.9 ml	10.9					
4	F	29	**6.90**	**9.03**	**17.33**	**8.10**	**8.24**					
			65.5	28.3	7.2	4.3 ml	11.0					
5	F	21	**6.46**	**3.98**	**15.37**	**6.22**	**7.91**					
			82.0	20.9	8.6	6.0 ml	10.4					
6	M	22	**6.42**	**14.4**	**32.30**	**10.03**	**4.20**					
			55.0	19.4	7.3	6.2 ml	12.6					
7	F	29	**6.40**	**5.33**	**6.56**	**10.12**	**7.63**					
			49.9	11.6	7.4	4.7 ml	12.0					
8	F	27	**5.19**	**12.4**	**12.71**	**-**	**6.49**					
			56.7	12.5	5.3	-	10.7					
9	F	26	**9.39**	**6.73**	**18.88**	**13.56**	**16.30**					
			35.6	10.7	7.3	2.6 ml	8.7					
10	F	30	**11.67**	**11.0**	**12.75**	**7.27**	**10.63**					
			55.8	15.7	5.7	5.5 ml	8.6					
11	M	28	**4.58**	**9.46**	**21.30**	**5.97**	**21.12**					
			54.3	19.1	9.1	5.3 ml	9.2					
12	M	36	**9.32**	**11.2**		**9.39**	**9.78**	**-**	**7.34**	**23.14**	**32.84**	**8.19**
			41.7	22.9		6.2 ml	4.8	-	12.6	2.2	1.8 ml	7.3 ml
13	M	33	**8.09**	**33.5**		**12.07**	**14.25**	**-**	**8.42**	**27.25**	**46.06**	**13.91**
			22.6	18.7		5.5 ml	7.0	-	10.3	1.2	1.4 ml	6.9 ml
14	M	33	**10.15**	**7.47**		**11.96**	**12.43**	**40.66**	**18.46**	**26.78**	**24.71**	**7.88**
			34.5	20.0		5.6 ml	7.9	2.3 ml	12.9	0.7	3.1 ml	7.3 ml
15	M	29	**6.03**	**8.75**		**12.27**	**14.15**	**16.46**	**6.73**	**579.7**	**20.37**	**10.99**
			43.7	22.2		6.4 ml	6.6	3.9 ml	12.5	0.9	3.1 ml	5.3 ml
16	M	31	**4.95**	**4.20**		**5.94**	**4.19**	**28.57**	**5.00**	**19.96**	**19.23**	**10.32**
			46.9	16.5		6.1 ml	8.3	2.7 ml	12.0	1.2	3.3 ml	6.5 ml

Graphical abstract

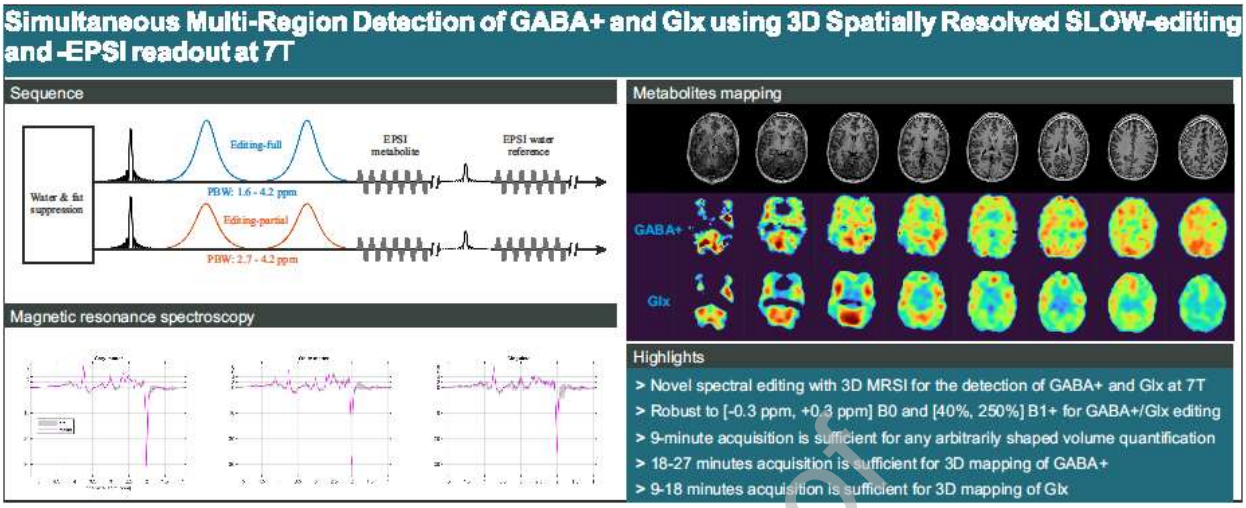

Declaration of Competing Interest

Guodong Weng and Johannes Slotboom disclose that the application of SLOW-editing described in the paper has been filed at the International Bureau of WIPO as a PCT patent application.

Patent applicant: Universität Bern.

Status of application: published (WO 2022/229728).

Inventors: Guodong Weng and Johannes Slotboom